THE JOURNAL OF BIOLOGICAL CHEMISTRY VOL. 289, NO. 11, pp. 7835–7843, March 14, 2014

Iron Regulatory Protein-1 Protects against Mitoferrin-1-deficient Porphyria*

Received for publication, January 16, 2014 Published, JBC Papers in Press, February 7, 2014, DOI 10.1074/jbc.M114.547778

Jacky Chung[‡], Sheila A. Anderson[§1], Babette Gwynn[¶1], Kathryn M. Deck[§], Michael J. Chen[‖], Nathaniel B. Langer[‡2], George C. Shaw[‡3], Nicholas C. Huston[‡], Leah F. Boyer[‖4], Sumon Datta[‖5], Prasad N. Paradkar[6], Liangtao Li[**], Zong Wei[‡‡7], Amy J. Lambert[¶], Kenneth Sahr[¶], Johannes G. Wittig[‡8], Wen Chen[‡9], Wange Lu[‡‡], Bruno Galy[§§], Thorsten M. Schlaeger[‖], Matthias W. Hentze[§§], Diane M. Ward[**], Jerry Kaplan[**], Richard S. Eisenstein[§], Luanne L. Peters[¶10], and Barry H. Paw[‡11]**

*From the [‡]Division of Hematology, Brigham and Women's Hospital; Division of Hematology-Oncology, Boston Children's Hospital and Harvard Medical School, Boston, Massachusetts 02115, the [§]Department of Nutritional Sciences, University of Wisconsin-Madison, Madison, Wisconsin 53706, [¶]The Jackson Laboratory, Bar Harbor, Maine 04609, the [‖]Stem Cell Program, Boston Children's Hospital, Harvard Medical School, Boston, Massachusetts 02115, the **Department of Pathology, University of Utah School of Medicine, Salt Lake City, Utah 84132, the [‡‡]Department of Biochemistry and Molecular Biology, Eli and Edythe Broad Center for Regenerative Medicine and Stem Cell Research and Keck School of Medicine, University of Southern California, Los Angeles, California 90089, and the [§§]European Molecular Biology Laboratory, D-69117 Heidelberg, Germany*

Background: Heme and [Fe-S] cluster assembly are tightly regulated processes that require mitochondrial iron.
Results: Loss of mitochondrial iron activates the [Fe-S]-dependent RNA-binding activity of IRP1 that inhibits protoporphyrin biosynthesis.
Conclusion: IRP1 forms a critical feedback mechanism, preventing protoporphyrin accumulation under limiting mitochondrial iron conditions.
Significance: This study provides evidence linking heme biogenesis to that of [Fe-S] clusters synthesis.

Mitochondrial iron is essential for the biosynthesis of heme and iron-sulfur ([Fe-S]) clusters in mammalian cells. In developing erythrocytes, iron is imported into the mitochondria by MFRN1 (mitoferrin-1, SLC25A37). Although loss of MFRN1 in zebrafish and mice leads to profound anemia, mutant animals showed no overt signs of porphyria, suggesting that mitochondrial iron deficiency does not result in an accumulation of protoporphyrins. Here, we developed a gene trap model to provide *in vitro* and *in vivo* evidence that iron regulatory protein-1 (IRP1) inhibits protoporphyrin accumulation. $Mfrn1^{+/gt}$; $Irp1^{-/-}$ erythroid cells exhibit a significant increase in protoporphyrin levels. IRP1 attenuates protoporphyrin biosynthesis by binding to the 5′-iron response element (IRE) of *alas2* mRNA, inhibiting its translation. Ectopic expression of *alas2* harboring a mutant IRE, preventing IRP1 binding, in $Mfrn1^{gt/gt}$ cells mimics *Irp1* deficiency. Together, our data support a model whereby impaired mitochondrial [Fe-S] cluster biogenesis in $Mfrn1^{gt/gt}$ cells results in elevated IRP1 RNA-binding that attenuates ALAS2 mRNA translation and protoporphyrin accumulation.

* This work was supported by grants from the American Society of Hematology (to G. C. S.), the Canadian Institutes of Health Research (CIHR postdoctoral fellowship (to J. C.), the Federal Ministry of Education and Research (BMBF, Virtual Liver (to M. W. H.), the March of Dimes Foundation (6-FY09-289) (to B. H. P.), and the National Institutes of Health R01 HL088468 (to L. L. P.), R01 DK052380 (to J. K.), R01 DK066600 (to R. S. E.), and R01 DK070838 and P01 HL032262 (to B. H. P.).
[1] Both authors contributed equally to this work.
[2] Present address: Columbia University College of Physicians and Surgeons, NY, NY 10032.
[3] Present address: University of Pennsylvania School of Medicine, Philadelphia, PA 19104.
[4] Present address: University of California, San Diego, La Jolla, CA 92093.
[5] Present address: Novartis, Cambridge, MA 02139.
[6] Present address: The Commonwealth Scientific and Industrial Research Organisation, Clayton, Victoria 3169, Australia.
[7] Present address: Salk Institute for Biological Studies, La Jolla, CA 92037.
[8] Present address: Brandenburgische Technische Universität Cottbus-Senftenberg, 01968 Senftenberg, Germany.
[9] Present address: Texas A&M Health Science Center, Temple, TX 76508.
[10] To whom correspondence may be addressed: The Jackson Laboratory, 600 Main St., Bar Harbor, ME 04609. Tel.: 207-288-6391; Fax: 207-288-6073; E-mail: luanne.peters@jax.org.
[11] To whom correspondence may be addressed: Div. of Hematology, Brigham and Women's Hospital, 1 Blackfan Cir., Karp Research Bldg. 05.211, Boston, MA 02115. Tel.: 617-355-9008; Fax: 617-355-9064; E-mail: bpaw@rics.bwh.harvard.edu.

Iron is an essential element that is incorporated into prosthetic groups that function in a multitude of biochemical processes. Two of these iron-containing prosthetic groups are heme and iron-sulfur ([Fe-S]) clusters. Heme is a moiety with diverse functions in many cell types and is an integral component of hemoglobin in erythroid cells (1). [Fe-S] clusters are requisite cofactors for many enzymes, including aconitases and succinate dehydrogenase (2, 3). Although functionally distinct, assembly of both cofactors require mitochondrial function and mitochondrial iron assimilation (4).

Iron is imported into mitochondria via two transporters: mitoferrin-1 (MFRN1, SLC25A37) and mitoferrin-2 (MFRN2, SLC25A28). MFRN2 is expressed ubiquitously, whereas MFRN1 is specifically induced in differentiating erythroid cells (5–7). Previous work has shown that loss of *Mfrn1* in *frascati* zebrafish and mice disrupts heme and [Fe-S] cluster synthesis, owing to a severe reduction in mitochondrial iron in erythroid progenitors (7, 8). However, neither $Mfrn1^{-/-}$ mice nor

zebrafish *frascati* embryos deficient in *Mfrn1* develop porphyria. In fact, conditional deletion of *Mfrn1* in hepatocytes only causes porphyria and hepatobiliary stasis when the animals are fed a δ-aminolevulinic acid (ALA)-rich[12] diet (8). This indicates that reduction in mitochondrial iron stores may concomitantly attenuate early steps of protoporphyrin synthesis.

Recent evidence suggests that cross-talk between [Fe-S] cluster assembly and protoporphyrin synthesis pathways may explain the absence of porphyria in $Mfrn1^{-/-}$ animals (9). Cellular iron homeostasis is largely regulated by iron regulatory proteins-1 (IRP1) and -2 (IRP2) that can directly influence protein expression via two mechanisms (10–12). IRPs can bind to iron responsive elements (IREs) in the 5′-UTRs of mRNAs, blocking translation initiation. Alternatively, mRNAs with IRE(s) in the 3′-UTR have increased stability when bound by IRPs. As a result, this latter class of transcripts will have increased accumulation when IRPs are activated by iron deficiency. Although IRP1 and IRP2 exhibit some functional redundancy and can be regulated by common mechanisms (13–15), IRP1 is unique in that RNA-binding activity is negatively regulated by [Fe-S] cluster biogenesis. Insertion of an [Fe-S] cluster into IRP1 converts IRP1 from an IRE-RNA binding protein to cytosolic aconitase (ACO1). A decline in [Fe-S] cluster synthesis would, therefore, trigger increased IRP1 RNA-binding activity (16–19).

One mRNA harboring a 5′-IRE is erythroid-specific aminolevulinate synthase 2 (*Alas2*), which encodes the enzyme that catalyzes the first step in the heme biosynthetic pathway (20, 21). Wingert and colleagues (9) previously demonstrated that inhibition of glutaredoxin 5 (*Glrx5*), a gene required for mitochondrial [Fe-S] cluster assembly, resulted in anemia in zebrafish via increased IRP1-mediated inhibition of ALAS2 translation. Thus, a reduction in [Fe-S] cluster assembly in response to iron deficiency can feedback to attenuate the very proximal step of heme assembly (9, 22). Here, we examined whether loss of *Mfrn1* can also trigger IRP1 activity in erythroid cells. We generated a model to show that in the absence of MFRN1, IRP1 blocks ALAS2 translation, preventing the accumulation of protoporphyrins *in vitro* and *in vivo*. Loss of IRP1 or the 5′-IRE in *Alas2* mRNA resulted in porphyria. Our work indicates that IRP1 functions as a critical link coupling heme and [Fe-S] cluster biosynthetic pathways and that in the absence of MFRN1-mediated mitochondrial iron import, IRP1 protects erythroid cells against porphyria.

EXPERIMENTAL PROCEDURES

Cell Culture—Friend murine erythroleukemia cells were cultured and differentiated as described previously (23). Mouse embryonic stem (mES) cells containing a gene trap insertion in *Mfrn1* ($Mfrn1^{+/gt}$ cell line, XB454, derived from strain 129P2) were obtained from the University of California, San Francisco BayGenomics (24). Insertion of the gene trap vector (containing the coding sequence for β-geo) into *Mfrn1* was verified by direct sequencing of cDNA obtained by 5′-rapid amplification of cDNA ends (25). mES cells were maintained on gelatin-coated 100-mm dishes in mES cell medium (7). Null $Mfrn1^{gt/gt}$ mES clones were derived using G418 selection as described previously (7).

Mouse Blastocyst Injections and Knock-out Mouse Creation—ES cells were injected into C57BL/6J blastocysts and transferred to pseudopregnant C57BL/6J hosts using standard techniques (26). Male chimeras identified by *agouti* coat color were mated to C57BL/6J females to generate heterozygotes for interbreeding to produce homozygous knock-out progeny. Progeny were genotyped as described below. All mice were maintained at The Jackson Laboratory in a climate-controlled room with a 12-h light cycle and provided acidified water and NIH 5K52 chow *ad libitum*. The Jackson Laboratory Animal Care and Use Committee approved all protocols. In accordance with the International Committee on Standardized Genetic Nomenclature for Mice, the official genetic designation for this *Mfrn1* targets strain is B6.129P2-Slc25a37<Gt(XB454)Byg>/Llp.

Mouse Genotyping—For analysis by Southern blotting, HindIII-digested mouse genomic or ES cell DNA was transferred onto Hybond Nylon (Amersham Biosciences), and probed with random primed labeled [α-^{32}P]dCTP (3000 Ci/mmol; New England Nuclear) murine *Mfrn1* or *Escherichia coli lacZ* cDNA under standard hybridization and washing conditions. Genotyping by PCR on genomic DNA was performed with the following primer pairs and resolved on a 5% native polyacrylamide gel:

The following were used in this work: for the wild-type allele (269-bp fragment), 5′-GCTTATGGAAAGGAACCCAGCC-3′ (F1 primer) and 5′-ACAAGGAAGAGCCAGGACTGTCAG-3′ (R1 primer); mutant *gt* allele (350-bp fragment) as shown above (F1 primer) and 5′-CGCCATACAGTCCTCTTCACAT-3′ (R2 primer); LacZ, 5′-TTATCGATGAGCGTGGTGGTTATGC-3′ (F primer) and 5′-GCGCGTACATCGGGCAAATAATATC-3′ (R primer). Primers for *Irp1* mutant mice were as described previously (27).

LacZ Staining—β-Galactosidase staining of mouse embryos was performed as described previously (7).

Mixed Chimera Analysis—$Mfrn1^{gt/gt}$ ES cell clones were injected into C57BL/6J mouse blastocysts and transferred to C57BL/6J recipients. The degree of mosaicism in offspring was estimated by coat color. The contributions of donor (129P2) *versus* recipient (C57BL/6) ES cells to the red cell and leukocyte compartments were determined by cellulose acetate electrophoresis to detect strain-specific hemoglobin and glucose-6-isomerase alleles as described previously (28) in three chimeric mice (one female with moderate chimerism, two males with moderate to high chimerism) at 10 weeks of age.

o-Dianisidine Staining, CFU-E, and Cytospin Assays—Wild-type E14 and *Mfrn1* null ES clones were generally split 1 day after thawing with 10^6 mES cells plated onto gelatinized 100-mm plates in mES media as described previously (7). The following day, mES cells were maintained in "switch media" (7). Two days after the split, the cells were collected by trypsinization and replated on untreated 100-mm dishes at a density of 3×10^3 cells/ml (total 6×10^4 cells) in embryoid body (EB) media with murine VEGF (10 ng/ml) on days 1 and 5. ALA (0.25

[12] The abbreviations used are: ALA, δ-aminolevulinic acid; ES, embryonic stem; PPIX, protoporphyrin IX; [Fe-S], iron-sulfur; IRE, iron-response element; IRP1, iron regulatory protein-1; Alas2, aminolevulinate synthase 2; E1, embryonic day 1; EB, embryoid body; FECH, ferrochelatase.

mM) was added to EB cultures for the last 24 h of day 6 primitive differentiation (7). Hemoglobinization of the primitive differentiated cells was assessed by *o*-dianisidine staining as described (29).

To achieve definitive hematopoietic differentiation, the EB medium was supplemented with mVEGF (10 ng/ml), rEPO (10 international units/ml), mSCF (5 ng/ml). Day 5 EBs were supplemented with recombinant erythropoietin (5 units/ml), mIL-3 (5 ng/ml), mIL-6 (10 ng/ml), and mSCF (100 ng/ml) and harvested on day 6. mEBs were disaggregated by trituration in 0.25% trypsin via an 18-gauge syringe. The disaggregated EBs were replated in three-dimensional methylcellulose culture for CFU-E analysis (7). Picked CFU-Es were morphologically analyzed by cytospin and Wright-Giemsa staining (7).

Semi-quantitative RT-PCR for Erythroid Markers—Total RNA was isolated from ~10^5 differentiated cells from wild-type (*Mfrn1*$^{+/+}$), heterozygous (*Mfrn1*$^{+/gt}$), and null (*Mfrn1*$^{gt/gt}$) embryoid bodies on day 6 using the Qiagen RNasy kit. cDNA was synthesized using random hexamers with Superscript II reverse transcriptase (Invitrogen). PCR was performed with [α-^{32}P]dCTP (3000 Ci/mmol; New England Nuclear) and Platinum TaqDNA polymerase (Roche Applied Science) under standard conditions for 30–32 cycles. PCR products were resolved on a 5% native polyacrylamide gel, treated in 10% methanol:acetic acid fixative, dried, and exposed to autoradiography. The following murine gene-specific primers were used for semi-quantitative RT-PCR: *Mfrn1*, 5′-AGCTGTGTGGTGTAACTCCTGTAG-3′ (forward) and 5′-AGGACTTTAAATGACGTTTTCAGC-3′ (reverse); *Mfrn2*, 5′-GCCCACGCCCTCTATTTTG-3′ and 5′-CGGCGTGGCGGGAGGAC-3′; β-major globin, 5′-GGTTTAGTGGTACTTGTGAGCC-3′ and 5′-ATGGTGCACCTGACTGATGCTG-3′; βH1 globin, 5′-AGTCCCCATGGAGTCAAAGA-3′ and 5′-CTCAAGGAGACCTTTGCTCA-3′; α-globin, 5′-TGGCTAGCCAAGGTCACCAGC-3′ and 5′-CTCTCTGGGAAGACAAAAGCAAC-3′; *Alas2*, 5′-GATCCAAGGCATTCGCAACA-3′ and 5′-GATGGCCTGCACATAGATGC-3′; *Gata-1*, 5′-ACTCGTCATACCACTAAGGT-3′ and 5′-AGTGTCTGTAGGCCTCAGCT-3′; *Dmt1*, 5′-GGTTCTGACATGCAGGAAGT-3′ and 5′-CAAAGACATTGATGATGAAG-3′; *Hprt*, 5′-CACAGGACTAGAACACCTGC-3′ and 5′-GCTGGTGAAAAGGACCTCT-3′; and GAPDH, 5′-TGATGACATCAAGAAGGTGGTGAAG-3′ and 5′-TCCTTGGAGGCCATGTAGGCCAT-3′.

Iron, Heme, and Protoporphyrin Assays—Intracellular iron measurement was performed as described previously (30). Cells were washed in nitric acid, and sample iron content was determined using a Perkin-Elmer inductively coupled plasma optical emission spectrometer. Results were normalized by cell numbers. Mitochondrial iron was similarly quantitated by inductively coupled plasma spectroscopy in mitochondria that were isolated from wild-type *Mfrn1*$^{+/+}$ or *Mfrn1*$^{gt/gt}$ EBs using the mitochondrial isolation kit according to the manufacturer's instructions (Promega, Madison, WI) and normalized by mitochondrial protein content. For heme and protoporphyrin assays, EBs or embryos were sonicated and heme and protoporphyrin were extracted in 19:1 acetone:concentrated HCl as described (31). The resulting supernatant was injected immediately into a computer-controlled Waters reverse phase high-pressure liquid chromatography system that consisted of a 996 Photodiode Array Detector, a 474 scanning fluorescence detector, an AllianceHT 2795 separations module, and a μBondapak C18 3.9 × 300 mm column with a guard column attached. Bovine Type 1 crystalline heme (Sigma, H-2250) or Protoporphyrin IX (Sigma, P-8293) was used as the standard. The absorbance values were normalized by cell number or protein concentration. EBs were supplemented with 0.25 mM ALA (Sigma) for 24 h prior to cell harvest and biochemical analysis.

Western Analysis—Immunoblotting was performed as described previously (32). Custom, affinity-purified anti-mouse MFRN1 rabbit polyclonal antibody was generated using the following peptide: C-HESHVQEVSHKTSPT (Genemed Synthesis, San Antonio, TX). Goat polyclonal anti-HSP60 (K-19) was purchased from Santa Cruz Biotechnology. Anti-ALAS2 was a generous gift of Dr. Makoto Murakami (Tokyo Metropolitan Institute of Medical Science, Tokyo, Japan). Quantitative densitometry was performed using ImageJ software (NIH, Bethesda, MD) and normalized to HSP60 expression levels.

Zebrafish alas2 Expression Constructs—Wild-type zebrafish *alas2* cDNA with the 5′-IRE (+IRE; GenBank™ accession no. NM_131682.2) was subcloned into the BamHI/XhoI sites of pCS2+ as described previously (33). The *alas2* cDNA lacking the 5′-IRE (−IRE; 5′-GTTCGTCCTCAGTGCAGGTCAAC-3′) was amplified from this construct by PCR and subcloned into pCS2+. The *alas2* cDNA lacking the 5′-IRE with a premature nonsense mutation at amino acid residue 26 (Y26X), (−IRE/Stop), was generated using the QuikChange site-directed mutagenesis kit (Stratagene, La Jolla, CA). These clones were subsequently subcloned into MluI/XhoI sites in the pMMP-HA-IRES-eGFP retroviral vector (34) for subsequent lentivirus production.

Lentivirus Infection—Lentivirus production and infection was performed as described previously (35). Briefly, 293T cells were plated at 6 × 10^6 cells per 100 mm dish and incubated overnight. Cells were transfected with retroviral vectors together with psPax2 and pMD2G. Forty-eight hours after transfection, the supernatants were collected and ultra-centrifuged at 28,000 rpm for 2 h. Supernatants from three 10-cm dishes were concentrated into 100 μl of PBS. Murine ES cells in 24-well plates were transduced using various amounts of concentrated virus supplemented with 8 μg/ml polybrene. After 24 h, the cells were changed back to standard medium. Three days after transduction, the cells were dissociated by 0.05% trypsin and sorted by FACS to obtain the GFP-positive cells.

Mouse Matings between Mfrn1 and Irp1 Mice—Mfrn1$^{+/gt}$ mice were crossed with Irp1$^{+/-}$ mice (27, 36). *Mfrn1*$^{+/gt}$;*Irp1*$^{+/-}$ offspring were intercrossed to produce *Mfrn1*$^{+/gt}$;*Irp1*$^{-/-}$ and *Mfrn1*$^{+/gt}$;*Irp*$^{+/+}$ sires and dams. Embryos from mating *Mfrn1*$^{+/gt}$;*Irp1*$^{-/-}$ sires and dams, and embryos from mating *Mfrn1*$^{+/gt}$;*Irp1*$^{+/+}$ sires and dams were harvested at E10.5. After removing heads for genotyping, the remaining tissue was homogenized in 20 mM HEPES (4-(2-hydroxyethyl)-1-piperazineethanesulfonic acid) pH 7.5, buffer for heme and protoporphyrin analysis. All use of animals met the requirements of the University of Wisconsin-Madison Institutional Animal Care and Use Committee.

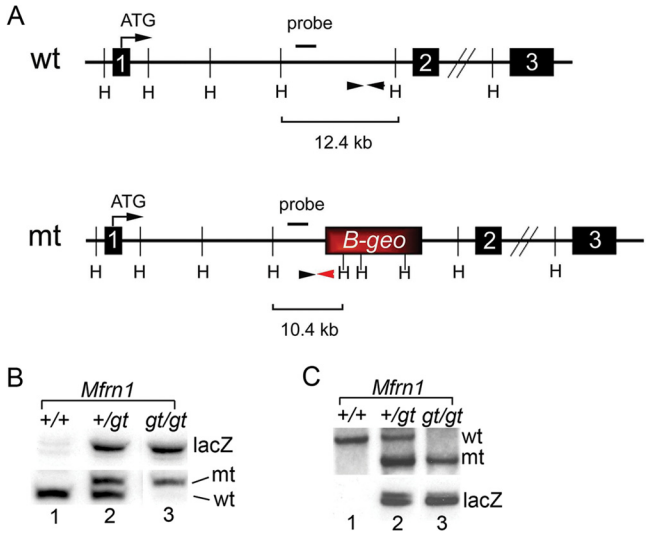

FIGURE 1. **Genomic organization and genotyping of the MFRN1 gene trap mES clone.** *A*, the wild-type (*wt*) and *Mfrn1* mutant (*mt*) gene trap alleles are shown, including the site of the β-geo cassette and the primer sites used for PCR genotyping (*black arrowheads*). The primer-specific for the β-geo cassette is denoted by a *red arrowhead*. The location of the probe used for Southern blotting as well as the HindIII sites (*H*) are also shown. *B* and *C*, genomic DNA was isolated from $Mfrn1^{+/+}$, $Mfrn1^{+/gt}$, and $Mfrn1^{gt/gt}$ ES cells following step-up selection and subjected to PCR (*B*) or Southern blot analysis (*C*) to confirm their genotypes.

RESULTS

$Mfrn1^{gt/gt}$ ES Cells Are Defective at Erythroid Differentiation—*Mfrn1* has been studied previously in mice using tissue-specific Cre/Lox technology (8). Although global loss of *Mfrn1* in this model leads to embryonic lethality due to a profound embryonic anemia, a cell-autonomous role for MFRN1 in adult hematopoiesis has never been described. Thus, to address this and to study the underlying molecular mechanisms, we developed a model where we could manipulate MFRN1 function *in vitro* and *in vivo*. Gene trap mutagenesis was used to disrupt the *Mfrn1* locus between introns 1 and 2 (Fig. 1*A*). Proper integration in murine ES cells was confirmed using PCR and Southern blot analysis (Fig. 1, *B* and *C*). Wild-type ($Mfrn1^{+/+}$), heterozygote ($Mfrn1^{+/gt}$), and null ($Mfrn1^{gt/gt}$) ES cells were then cultured *in vitro* under conditions that facilitate primitive or definitive erythropoiesis. $Mfrn1^{gt/gt}$ cells, lacking MFRN1 protein expression, showed defective hemoglobinization, failed to form both primitive and definitive CFU-E colonies and were morphologically distinct from wild-type differentiated erythroid cells (Fig. 2, *A–E*). Semi-quantitative RT-PCR analysis also revealed that expression of erythroid markers, α-globin, βH1-globin, βmajor-globin, and *Alas2*, were diminished in differentiating $Mfrn1^{gt/gt}$ cells compared with wild-type (Fig. 2*F*), indicating that erythroid maturation in mutant cells was blocked. In contrast, the early erythroid marker, *Gata-1*, and ubiquitously expressed genes such as *Mfrn2*, *Hprt*, and GAPDH were normal compared with wild-type and $Mfrn1^{+/gt}$ cells. Total intracellular iron, mitochondrial iron, and intracellular heme content were all decreased without protoporphyrin accumulation (Fig. 2, *G–I*, and data not shown). We also examined both endogenous aconitase 1 activity and IRP1 RNA-binding (data not shown). However, we were unable to detect significant changes using either assays with this embryoid culture system. We believe that this is due to a heterogeneous population of cells in our differentiation cultures. Under optimal conditions, only 30% of ES cells undergo proper erythroid maturation (Fig. 2*C*). RNA-binding and aconitase assays may lack sufficient sensitivity to detect moderate changes.

Mfrn1 Is Required for Primitive and Definitive Erythropoiesis in Vivo—We next examined whether the primitive erythropoietic defects in ES cells can be recapitulated *in vivo* by injecting wild-type or $Mfrn1^{gt/gt}$ ES cells into early-stage embryos and generating mixed-chimeric mice. $Mfrn1^{+/gt}$ and $Mfrn1^{gt/gt}$ offspring were obtained following germ line transmission of the mutant allele. Surrogate lacZ-staining for *Mfrn1* expression in heterozygote and gene-trapped embryos detected staining in the yolk sac blood islands and fetal liver at E8.5 and E11.5, respectively (Fig. 3, *A* and *B*). At E11.5, $Mfrn1^{gt/gt}$ embryos were severely anemic compared with wild-type littermates (Fig. 3*B*), and no mutant embryos survived past E11.5 (Table 1). MFRN1 is also required *in vivo* for definitive erythropoiesis. In mixed chimeras, only the host recipient C57BL/6J-derived hemoglobin isoform is detected by cellulose acetate electrophoresis of adult red cells (Fig. 3*C*). In contrast, genetic contributions from both recipient and donor (mutant, 129P2) glucose-6-isomerase isoforms were detected in leukocytes, indicating the essential role of MFRN1 in the development of the definitive erythroid lineage and its nonessential role in non-erythroid lineages in adult mice. These data confirm that our gene trap model provides an accurate representation of MFRN1 function *in vitro* and *in vivo*.

IRP1 Attenuates Protoporphyrin Production—Because disruption of [Fe-S] cluster synthesis has previously been linked to *Alas2* mRNA translational repression by IRP1 (9), we next used our model to ask whether ALAS2 translation had any influence on protoporphyrin production in the absence of MFRN1. $Mfrn1^{gt/gt}$ EBs had lower expression of ALAS2 protein compared with $Mfrn1^{+/+}$ EBs (Fig. 4*A*), suggesting that ALAS2 translation is indeed compromised in the absence of MFRN1. To examine the contribution of the 5′-IRE in MFRN1 regulation of ALAS2 function and expression, $Mfrn1^{gt/gt}$ ES cells were transduced with lentivirus expressing either empty vector (mock) or zebrafish *alas2* cDNA constructs harboring a wild-type IRE (WT) or mutant IRE (−IRE) in the 5′-UTR. An additional mutant *alas2* cDNA with a premature translational stop codon (−IRE/Stop) was also included as a negative control (Fig. 4, *B* and *C*). These cells were then differentiated into EBs. As expected, ectopic expression of WT-*alas2* resulted in a modest increase in protoporphyrin levels above mock-transduced control cells (Fig. 4, *C* and *D*). However, there was almost a 2-fold increase in protoporphyrin levels in cells expressing the −IRE mutant construct due to increased ALAS2 expression (Fig. 4, *C* and *D*). The level of protoprophyrin IX (PPIX) dropped to basal levels in cells expressing the double mutant *alas2* construct (−IRE/Stop) (Fig. 4, *C* and *D*). Furthermore, $Mfrn1^{gt/gt}$ EBs supplemented with exogenous ALA to by-pass the block in protoporphyrin synthesis resulting from diminished ALAS2 protein expression fully restored PPIX but not heme production to levels comparable with $Mfrn1^{+/+}$ cells (Fig. 4*E*). Thus, inhibition of protoporphyrin synthesis through action of the 5′-IRE in *Alas2* mRNA is substantially increased when mitochondrial

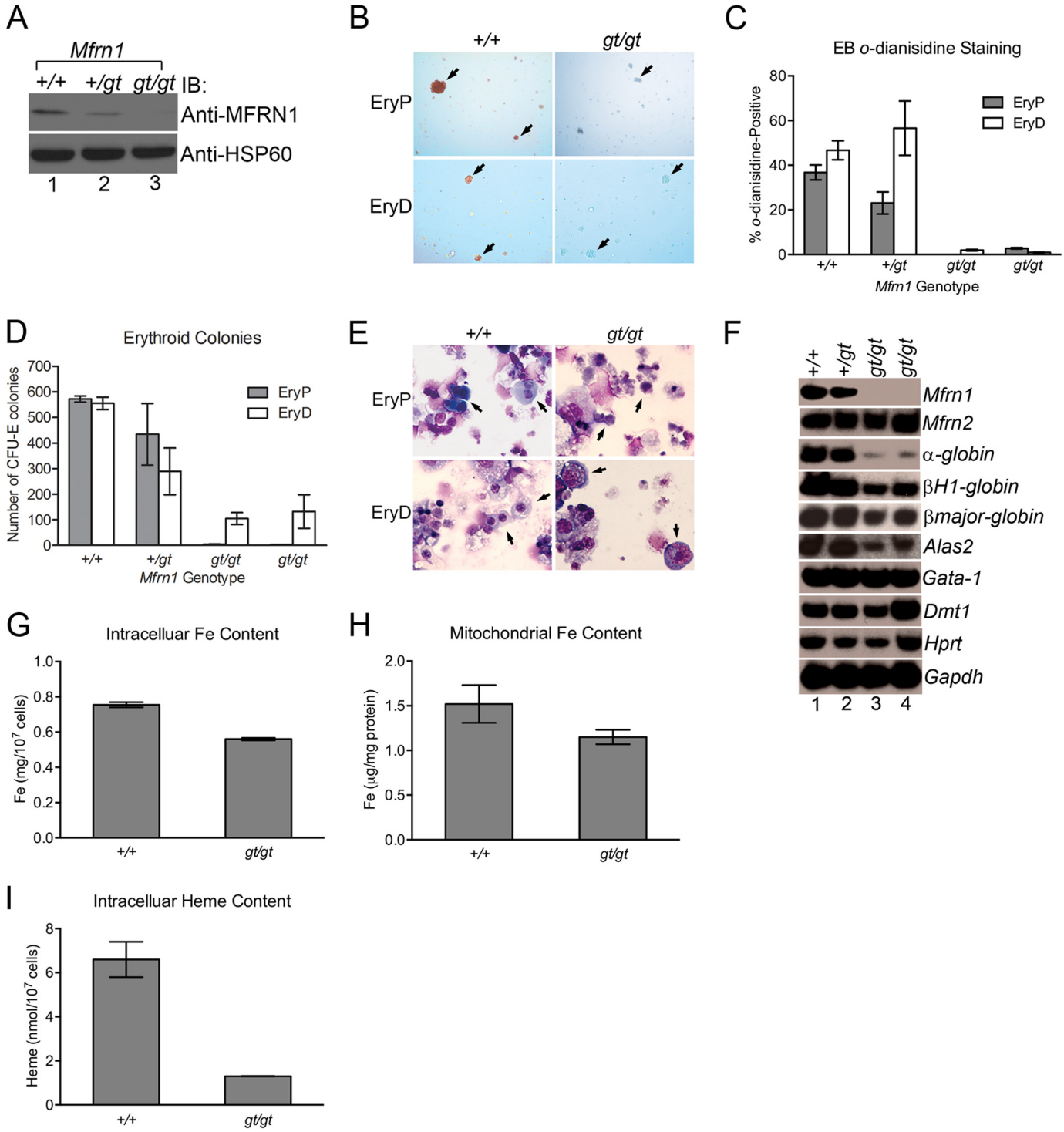

FIGURE 2. **Defect in hemoglobinization and maturation of primitive and definitive erythroblasts with Mfrn1 deficiency.** *A*, wild-type (+/+), heterozygote (+/*gt*), or *Mfrn1* gene-trap (*gt/gt*) ES cells undergoing primitive erythropoiesis were lysed and immunoblotted with anti-MFRN1 or anti-HSP60 antibodies, confirming the loss of Mfrn1 protein expression in *gt/gt* cells. *B* and *C*, EBs cultured under primitive (EryP) or definitive (EryD) conditions were analyzed for hemoglobinization by *o*-dianisidine staining using phase contrast microscopy (*B*) and quantified, showing a defect in hemoglobinization (*C*). The *arrows* denote cell clusters. *D*, quantitation of erythroid colonies (CFU-E) that formed under primitive or definitive conditions, showing defects on erythroid colony formation. *E*, primitive or definitive wild-type and gene trap cells were stained with Wright-Giemsa dye, showing maturation arrest of erythroblasts from *Mfrn1*$^{gt/gt}$ ES cells. *Arrows* denote representative erythroid cells. *Mfrn1*$^{+/+}$ cells are morphologically normal, whereas *Mfrn1*$^{gt/gt}$ cells have a larger nuclei. *F*, [α-^{32}P]dCTP-radiolabeled semi-quantitative RT-PCR analysis was performed on wild-type (+/+), heterozygote (+/*gt*), or two mutant (*gt/gt*) *Mfrn1* ES cell clones undergoing primitive differentiation using the indicated gene-specific primers. *G–I*, total intracellular iron (*Fe*; *G*), mitochondrial iron (*H*), and heme (*I*) content of *Mfrn1*$^{+/+}$ and *Mfrn1*$^{gt/gt}$ cells were examined, showing a consistent decrease in MFRN1-deficient embryoid bodies induced to undergo erythroid differentiation. Mean ± S.E. is shown, and all experiments were performed at least twice. *IB*, immunoblot.

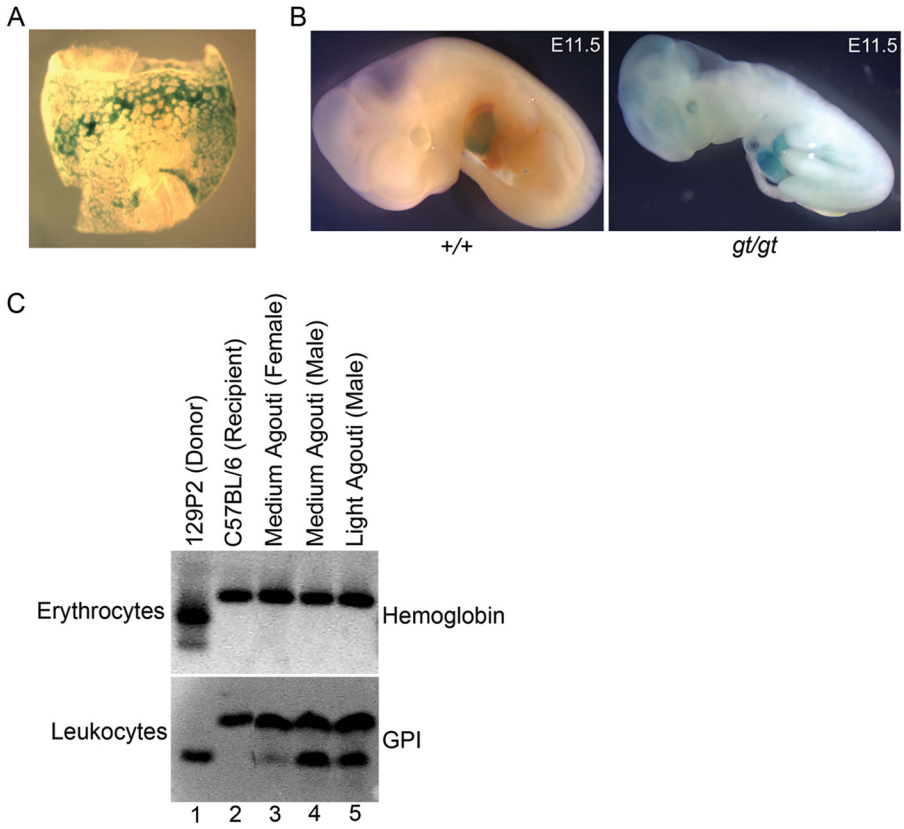

FIGURE 3. **MFRN1 is required for primitive and definitive erythropoiesis *in vivo*.** *A*, LacZ staining of gene trap *Mfrn1*$^{+/gt}$ E8.5 yolk sac, showing erythroid-specific expression in sites of hematopoiesis. *B*, gross morphology of E11.5 wild-type (+/+) or gene trap (*gt/gt*) embryos. The mutant embryos were also stained for lacZ and have a profound anemia due to a defect in primitive erythropoiesis. *C*, erythrocytes and leukocytes from recipient, donor, or chimeric mice with medium or light penetrance (agouti coat color) were isolated and lysed, and isoforms were resolved on starch-cellulose gel electrophoresis and Ponceau-red stained for hemoglobin or glucose-6-isomerase (*GPI*). MFRN1-deficient donor-derived cells do not contribute to adult erythrocytes but do contribute to the myeloid lineage, indicating that MFRN1 is dispensable for myelopoiesis.

TABLE 1
Number of *Mfrn1*$^{+/+}$, *Mfrn1*$^{+/gt}$, and *Mfrn1*$^{gt/gt}$ embryos during development

Developmental stage	Total no. of embryos	*Mfrn1*$^{+/+}$	*Mfrn1*$^{+/gt}$	*Mfrn1*$^{gt/gt}$
E8.5	30	8	12	10
E10.5	39	10	19	10
E11.5	9	1	6	2
E12.5	8	4	4	0
E14.5	24	8	16	0
E15.5	7	2	5	0

[Fe-S] cluster assembly is compromised. A deficiency of MFRN1 should result in elevated cytosolic IRP1 RNA-binding activity that would attenuate translation of ALAS2 and lower PPIX production and its intracellular accumulation.

To address whether this was the case *in vivo* and to confirm whether IRP1 was responsible for negatively regulating ALAS2 expression, we examined heme and protoporphyrin concentrations in four cohorts of murine embryos, *Mfrn1*$^{+/+}$;*Irp1*$^{+/+}$, *Mfrn1*$^{+/gt}$;*Irp1*$^{+/+}$, *Mfrn1*$^{+/+}$;*Irp1*$^{-/-}$, and *Mfrn1*$^{+/gt}$;*Irp1*$^{-/-}$, at E10.5. *Mfrn1* heterozygosity has little effect on heme levels in *Irp1*$^{+/+}$ background (Fig. 4*F*). Protoporphyrin levels decreased, consistent with the notion that a reduction in mitochondrial iron import, while having little effect on heme biosynthesis, activates IRP1 due to a mitochondrial [Fe-S] cluster biogenesis defect (7) to inhibit ALAS2 translation. It should be noted that ferrochelatase (FECH), the terminal and rate-limiting enzyme in heme biosynthesis, is a [Fe-S] cluster protein and would also be influenced by the ability to form [Fe-S] clusters (37). However, the decreased FECH activity is unlikely to be responsible for the decline in protoporphyrin levels because diminished FECH function is predicted to exacerbate protoporphyrin accumulation. In contrast, in the absence of IRP1, loss of one copy of *Mfrn1* causes a sharp rise in cellular protoporphyrin content, providing *in vivo* evidence that IRP1 prevents porphyria when MFRN1 is deficient. Taken together, our data strongly suggest that IRP1-mediated translational inhibition of ALAS2 in erythroid cells constitutes a feedback mechanism to attenuate protoporphyrin synthesis and accumulation when mitochondrial iron import through MFRN1 is compromised (Fig. 5).

DISCUSSION

The role of MFRN1 in primitive erythropoiesis and heme synthesis has been established in zebrafish and murine models (7, 8). Although these genetic studies have been highly informative, a cell-autonomous *in vivo* role for MFRN1 has never been described. It was also unclear as to why porphyria was never observed with MFRN1 deficiency. In this work, we developed a genetic and biochemical model to address these questions. We provide evidence that MFRN1 is essential for primitive and definitive erythropoiesis *in vivo*. These defects could be recapitulated in ES cell cultures, which allowed us to study the underlying

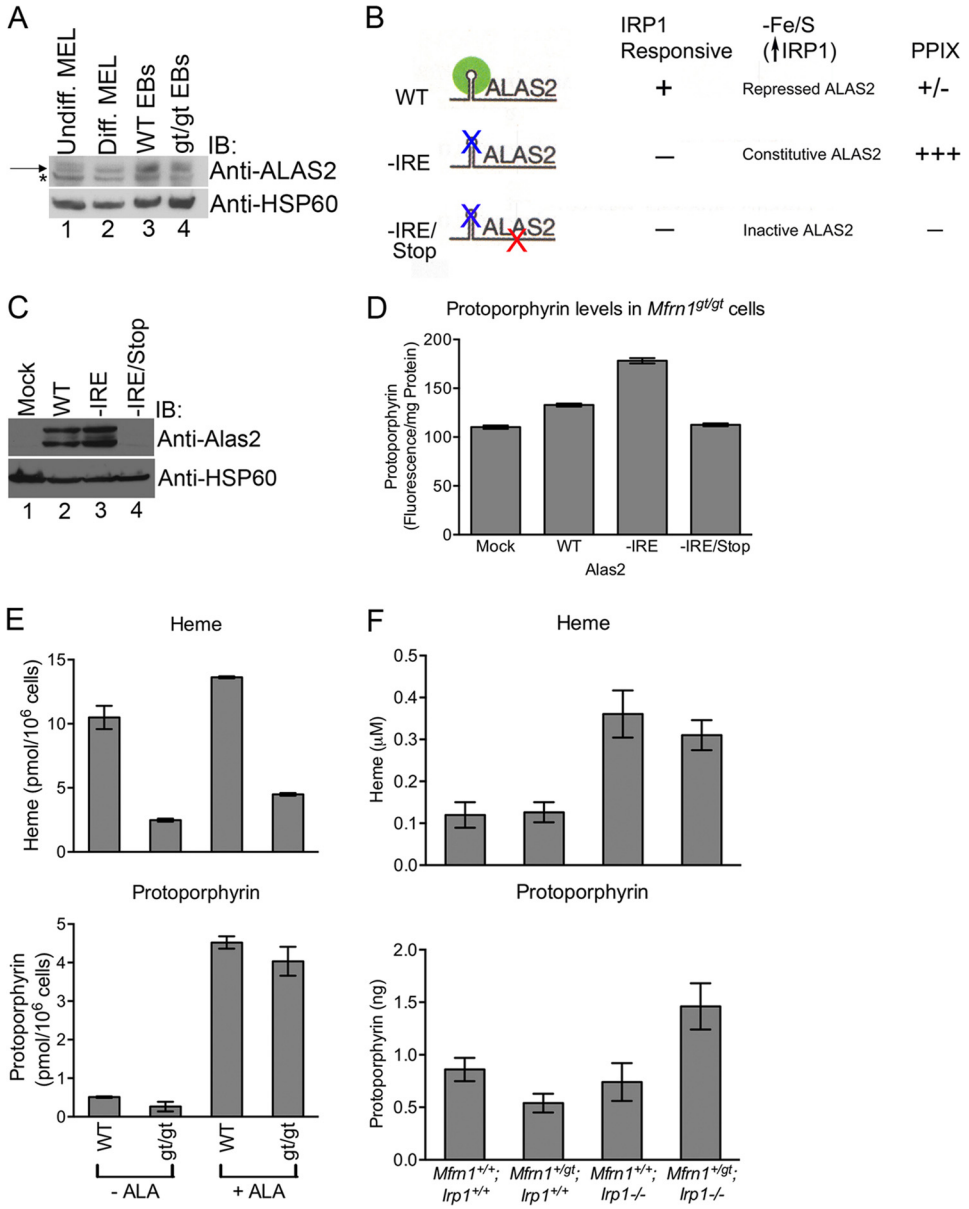

FIGURE 4. **Mitochondrial heme and Fe/S cluster biogenesis are co-regulated.** *A*, mitochondria were isolated from undifferentiated (*Undiff.*) and differentiated (*Diff.*) Friend murine erythroleukemia (*MEL*) cells as well as $Mfrn1^{+/+}$ and $Mfrn1^{gt/gt}$ embryoid bodies and subjected to Western blot analysis using the indicated antibodies. The *asterisk* denotes a cross-reacting band, and the *arrow* represents ALAS2. Densitometry analysis revealed that the intensities of the ALAS2 bands normalized to HSP60 expression levels in wild-type and $^{gt/gt}$ lanes are 100% and 61.5%, respectively. *B* and *C*, $Mfrn1^{gt/gt}$ ES cells infected with lentivirus expressing various *alas2* constructs were lysed, subjected to SDS-PAGE, and immunoblotted (*IB*) with anti-ALAS2 and anti-HSP60 antibodies. The schematic in *B* highlights the features of the *alas2* constructs as well as the anticipated results. *D*, PPIX levels were analyzed per milligram of total protein in $Mfrn1^{gt/gt}$ cells transduced with various lentiviruses, shown in *B*. *E*, heme and PPIX levels were measured in WT ($Mfrn1^{+/+}$) and $^{gt/gt}$ ($Mfrn1^{gt/gt}$) embryoid bodies with (+ALA) or without exogenous (−ALA), showing a dramatic increase in protoporphyrin but not heme in $Mfrn1^{gt/gt}$ cells because mitochondrial iron is limiting. *F*, murine embryos of various genotypes were examined for heme and protoporphyrin content at E10.5. Shown are mean ± S.E.; all experiments were performed at least twice. *IB*, immunoblot.

molecular mechanisms that couple mitochondrial iron homeostasis, heme metabolism, and [Fe-S] assembly. We demonstrate that IRP1 is a critical negative regulator of protoporphyrin synthesis in $Mfrn1^{gt/gt}$ erythroid cells via IRE-mediated repression of ALAS2 translation (Fig. 5). *Mfrn1* mutant embryos only developed porphyria in the absence of IRP1 (Fig. 4).

Although our studies have focused on IRP1, both IRP1 and IRP2 function in red blood cells to regulate ALAS2 translation (9, 17, 38). Studies of translational regulation of 5′-IRE-containing mRNA in a cell culture model of erythropoiesis found that unlike ferritin mRNA, which was almost totally translationally repressed, *Alas2* mRNA was partially repressed with significant amounts of the mRNA present on polyribosomes as well as in the translationally silent ribonucleoprotein pool (39). Thus, an erythropoietic phenotype tied to altered ALAS2 expression is predicted in response to either a reduction or an increase in IRP RNA-binding activity. $Irp2^{-/-}$ mice develop erythropoietic protoporphyria resulting from translational derepression of *Alas2* mRNA and subsequent overproduction of protoporphyrin intermediates (16, 17). In contrast, impairment of [Fe-S] cluster biogenesis when ABCB7 (40–42) or GLRX5 (9, 22) are disrupted specifically activates IRP1 RNA-

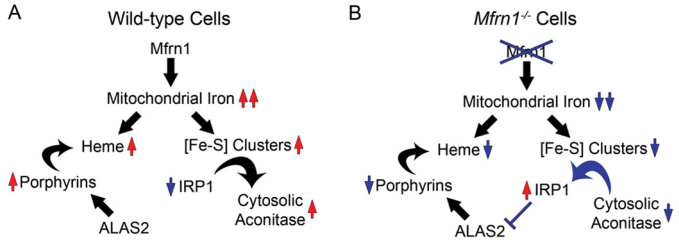

FIGURE 5. **Schematic model of mitochondrial heme and Fe/S cluster co-regulation.** *A*, MFRN1 imports iron into the mitochondria for heme and [Fe-S] cluster biosynthesis. When mitochondrial iron is readily available, sufficient [Fe-S] cluster synthesis converts IRP1 from an IRE-binding protein to cytosolic aconitase. *B*, however, when mitochondrial iron stores are compromised by MFRN1 mutation, both heme and [Fe-S] cluster syntheses are disrupted. Deficient [Fe-S] cluster availability results in activation of IRP1 that subsequently binds to IREs on target transcripts. IRP1 binding to the 5′-IRE of *Alas2* mRNA inhibits ALAS2 translation, thereby forming a feedback loop that attenuates protoporphyrin accumulation in the absence of mitochondrial iron.

binding activity leading to repression of *Alas2* mRNA translation. The observed increase in IRP1-mediated inhibition of ALAS2 via its 5′-IRE suggests that [Fe-S] cluster insertion into ACO1 is also compromised in the absence of MFRN1. Thus, by further supporting the concept that cytosolic [Fe-S] biogenesis is downstream of mitochondrial [Fe-S] formation that is fueled, in part, by the action of MFRN1, our findings also illustrate the unique role of IRP1 in linking mitochondrial iron metabolism with protoporphyrin synthesis in erythroid cells (9, 40, 43, 44). Taken together, these studies highlight differing roles of IRP1 and IRP2 in regulating ALAS2-IRP1 links protoporphyrin synthesis with [Fe-S] cluster synthesis and mitochondrial function, whereas IRP2 may have a more general "housekeeping" role in iron metabolism.

Our work presented here has important clinical implications. They suggest that although *Mfrn1* mutations may contribute to human porphyrias, *Mfrn1* inactivation alone is not likely sufficient for development of erythropoietic protoporphyria. In accord, expression of aberrant *Mfrn1* and a concomitant decrease in *Fech* expression is associated with human erythropoietic protoporphyria (45). Interestingly, C-terminal ALAS2-activating mutations (45–47) were also found in these erythropoietic protoporphyria patients with abnormal *Mfrn1* transcripts. Also, *Alas2* has been shown to be a genetic modifier in patients with congenital erythropoietic porphyria (48–50). This indicates that the IRP1/ALAS2 negative feedback loop also exists in humans and that disruption of multiple regulators in the heme and [Fe-S] cluster synthesis pathways are required for protoporphyrin accumulation (45). In *Mfrn1*$^{-/-}$ conditional knock-out mice, this porphyria effect can be recapitulated by exogenous chemical supplementation of ALA in the diets (8). Given the cytotoxic effects of protoporphyrin and its biosynthetic intermediates, the IRP1/ALAS2 feedback mechanism may have evolved in mammals to tightly link protoporphyrin synthesis with iron availability to guard against their deleterious overaccumulation.

Acknowledgments—We thank Drs. Yvette Yien and Caiyong Chen for insightful discussion. We thank Prof. Makoto Murakami (Tokyo Metropolitan Institute of Medical Science, Tokyo, Japan) for the anti-ALAS2 antisera. We also thank Christopher Nizzi (University of Wisconsin, Madison, WI) for preparation of the ^{32}*P-labeled RNA probe.*

REFERENCES

1. Schultz, I. J., Chen, C., Paw, B. H., and Hamza, I. (2010) Iron and porphyrin trafficking in heme biogenesis. *J. Biol. Chem.* **285,** 26753–26759
2. Rouault, T. A., and Tong, W. H. (2008) Iron-sulfur cluster biogenesis and human disease. *Trends Genet.* **24,** 398–407
3. Lill, R. (2009) Function and biogenesis of iron-sulphur proteins. *Nature* **460,** 831–838
4. Chung, J., Chen, C., and Paw, B. H. (2012) Heme metabolism and erythropoiesis. *Curr. Opin. Hematol.* **19,** 156–162
5. Amigo, J. D., Yu, M., Troadec, M. B., Gwynn, B., Cooney, J. D., Lambert, A. J., Chi, N. C., Weiss, M. J., Peters, L. L., Kaplan, J., Cantor, A. B., and Paw, B. H. (2011) Identification of distal cis-regulatory elements at mouse mitoferrin loci using zebrafish transgenesis. *Mol. Cell. Biol.* **31,** 1344–1356
6. Paradkar, P. N., Zumbrennen, K. B., Paw, B. H., Ward, D. M., and Kaplan, J. (2009) Regulation of mitochondrial iron import through differential turnover of mitoferrin 1 and mitoferrin 2. *Mol. Cell. Biol.* **29,** 1007–1016
7. Shaw, G. C., Cope, J. J., Li, L., Corson, K., Hersey, C., Ackermann, G. E., Gwynn, B., Lambert, A. J., Wingert, R. A., Traver, D., Trede, N. S., Barut, B. A., Zhou, Y., Minet, E., Donovan, A., Brownlie, A., Balzan, R., Weiss, M. J., Peters, L. L., Kaplan, J., Zon, L. I., and Paw, B. H. (2006) Mitoferrin is essential for erythroid iron assimilation. *Nature* **440,** 96–100
8. Troadec, M. B., Warner, D., Wallace, J., Thomas, K., Spangrude, G. J., Phillips, J., Khalimonchuk, O., Paw, B. H., Ward, D. M., and Kaplan, J. (2010) Targeted deletion of the mouse Mitoferrin1 gene: from anemia to protoporphyria. *Blood* **117,** 5494–5502
9. Wingert, R. A., Galloway, J. L., Barut, B., Foott, H., Fraenkel, P., Axe, J. L., Weber, G. J., Dooley, K., Davidson, A. J., Schmid, B., Schmidt, B., Paw, B. H., Shaw, G. C., Kingsley, P., Palis, J., Schubert, H., Chen, O., Kaplan, J., Zon, L. I., and Tübingen 2000 Screen Consortium (2005) Deficiency of glutaredoxin 5 reveals Fe-S clusters are required for vertebrate haem synthesis. *Nature* **436,** 1035–1039
10. Rouault, T. A. (2006) The role of iron regulatory proteins in mammalian iron homeostasis and disease. *Nat. Chem. Biol.* **2,** 406–414
11. Anderson, C. P., Shen, M., Eisenstein, R. S., and Leibold, E. A. (2012) Mammalian iron metabolism and its control by iron regulatory proteins. *Biochim. Biophys. Acta* **1823,** 1468–1483
12. Hentze, M. W., Muckenthaler, M. U., Galy, B., and Camaschella, C. (2010) Two to tango: regulation of mammalian iron metabolism. *Cell* **142,** 24–38
13. Rouault, T. A. (2009) Cell biology. An ancient gauge for iron. *Science* **326,** 676–677
14. Salahudeen, A. A., Thompson, J. W., Ruiz, J. C., Ma, H. W., Kinch, L. N., Li, Q., Grishin, N. V., and Bruick, R. K. (2009) An E3 ligase possessing an iron-responsive hemerythrin domain is a regulator of iron homeostasis. *Science* **326,** 722–726
15. Vashisht, A. A., Zumbrennen, K. B., Huang, X., Powers, D. N., Durazo, A., Sun, D., Bhaskaran, N., Persson, A., Uhlen, M., Sangfelt, O., Spruck, C., Leibold, E. A., and Wohlschlegel, J. A. (2009) Control of iron homeostasis by an iron-regulated ubiquitin ligase. *Science* **326,** 718–721
16. Galy, B., Ferring, D., Minana, B., Bell, O., Janser, H. G., Muckenthaler, M., Schümann, K., and Hentze, M. W. (2005) Altered body iron distribution and microcytosis in mice deficient in iron regulatory protein 2 (IRP2). *Blood* **106,** 2580–2589
17. Cooperman, S. S., Meyron-Holtz, E. G., Olivierre-Wilson, H., Ghosh, M. C., McConnell, J. P., and Rouault, T. A. (2005) Microcytic anemia, erythropoietic protoporphyria, and neurodegeneration in mice with targeted deletion of iron-regulatory protein 2. *Blood* **106,** 1084–1091
18. Meyron-Holtz, E. G., Ghosh, M. C., Iwai, K., LaVaute, T., Brazzolotto, X., Berger, U. V., Land, W., Ollivierre-Wilson, H., Grinberg, A., Love, P., and Rouault, T. A. (2004) Genetic ablations of iron regulatory proteins 1 and 2 reveal why iron regulatory protein 2 dominates iron homeostasis. *EMBO J.* **23,** 386–395
19. Clarke, S. L., Vasanthakumar, A., Anderson, S. A., Pondarré, C., Koh, C. M., Deck, K. M., Pitula, J. S., Epstein, C. J., Fleming, M. D., and Eisenstein, R. S. (2006) Iron-responsive degradation of iron-regulatory protein 1 does not require the Fe-S cluster. *EMBO J.* **25,** 544–553
20. Hamza, I., and Dailey, H. A. (2012) One ring to rule them all: trafficking of heme and heme synthesis intermediates in the metazoans. *Biochim. Bio-*

phys. Acta **1823,** 1617–1632
21. Dandekar, T., Stripecke, R., Gray, N. K., Goossen, B., Constable, A., Johansson, H. E., and Hentze, M. W. (1991) Identification of a novel iron-responsive element in murine and human erythroid δ-aminolevulinic acid synthase mRNA. *EMBO J.* **10,** 1903–1909
22. Ye, H., Jeong, S. Y., Ghosh, M. C., Kovtunovych, G., Silvestri, L., Ortillo, D., Uchida, N., Tisdale, J., Camaschella, C., and Rouault, T. A. (2010) Glutaredoxin 5 deficiency causes sideroblastic anemia by specifically impairing heme biosynthesis and depleting cytosolic iron in human erythroblasts. *J. Clin. Invest.* **120,** 1749–1761
23. Chen, C., Garcia-Santos, D., Ishikawa, Y., Seguin, A., Li, L., Fegan, K. H., Hildick-Smith, G. J., Shah, D. I., Cooney, J. D., Chen, W., King, M. J., Yien, Y. Y., Schultz, I. J., Anderson, H., Dalton, A. J., Freedman, M. L., Kingsley, P. D., Palis, J., Hattangadi, S. M., Lodish, H. F., Ward, D. M., Kaplan, J., Maeda, T., Ponka, P., and Paw, B. H. (2013) Snx3 regulates recycling of the transferrin receptor and iron assimilation. *Cell Metab.* **17,** 343–352
24. Stryke, D., Kawamoto, M., Huang, C. C., Johns, S. J., King, L. A., Harper, C. A., Meng, E. C., Lee, R. E., Yee, A., L'Italien, L., Chuang, P. T., Young, S. G., Skarnes, W. C., Babbitt, P. C., and Ferrin, T. E. (2003) BayGenomics: a resource of insertional mutations in mouse embryonic stem cells. *Nucleic Acids Res.* **31,** 278–281
25. Townley, D. J., Avery, B. J., Rosen, B., and Skarnes, W. C. (1997) Rapid sequence analysis of gene trap integrations to generate a resource of insertional mutations in mice. *Genome Res.* **7,** 293–298
26. Robertson, E. J. (1987) Teratocarcinomas and Embryonic Stem Cells: A Practical Approach. Oxford University Press, New York
27. Anderson, S. A., Nizzi, C. P., Chang, Y. I., Deck, K. M., Schmidt, P. J., Galy, B., Damnernsawad, A., Broman, A. T., Kendziorski, C., Hentze, M. W., Fleming, M. D., Zhang, J., and Eisenstein, R. S. (2013) The IRP1-HIF-2α axis coordinates iron and oxygen sensing with erythropoiesis and iron absorption. *Cell Metab.* **17,** 282–290
28. Chen, J., Astle, C. M., and Harrison, D. E. (2000) Genetic regulation of primitive hematopoietic stem cell senescence. *Exp. Hematol.* **28,** 442–450
29. Stachura, D. L., Reyes, J. R., Bartunek, P., Paw, B. H., Zon, L. I., and Traver, D. (2009) Zebrafish kidney stromal cell lines support multilineage hematopoiesis. *Blood* **114,** 279–289
30. Li, L., Chen, O. S., McVey Ward, D., and Kaplan, J. (2001) CCC1 is a transporter that mediates vacuolar iron storage in yeast. *J. Biol. Chem.* **276,** 29515–29519
31. Cook, J. D. (1980) *Iron*, Churchill Livingstone, New York
32. Shah, D. I., Takahashi-Makise, N., Cooney, J. D., Li, L., Schultz, I. J., Pierce, E. L., Narla, A., Seguin, A., Hattangadi, S. M., Medlock, A. E., Langer, N. B., Dailey, T. A., Hurst, S. N., Faccenda, D., Wiwczar, J. M., Heggers, S. K., Vogin, G., Chen, W., Chen, C., Campagna, D. R., Brugnara, C., Zhou, Y., Ebert, B. L., Danial, N. N., Fleming, M. D., Ward, D. M., Campanella, M., Dailey, H. A., Kaplan, J., and Paw, B. H. (2012) Mitochondrial Atpif1 regulates haem synthesis in developing erythroblasts. *Nature* **491,** 608–612
33. Brownlie, A., Donovan, A., Pratt, S. J., Paw, B. H., Oates, A. C., Brugnara, C., Witkowska, H. E., Sassa, S., and Zon, L. I. (1998) Positional cloning of the zebrafish sauternes gene: a model for congenital sideroblastic anaemia. *Nat. Genet.* **20,** 244–250
34. Woo, A. J., Moran, T. B., Schindler, Y. L., Choe, S. K., Langer, N. B., Sullivan, M. R., Fujiwara, Y., Paw, B. H., and Cantor, A. B. (2008) Identification of ZBP-89 as a novel GATA-1-associated transcription factor involved in megakaryocytic and erythroid development. *Mol. Cell. Biol.* **28,** 2675–2689
35. Chung, J., Lau, J., Cheng, L. S., Grant, R. I., Robinson, F., Ketela, T., Reis, P. P., Roche, O., Kamel-Reid, S., Moffat, J., Ohh, M., Perez-Ordonez, B., Kaplan, D. R., and Irwin, M. S. (2010) SATB2 augments ΔNp63α in head and neck squamous cell carcinoma. *EMBO Rep.* **11,** 777–783
36. Galy, B., Ferring, D., Benesova, M., Benes, V., and Hentze, M. W. (2004) Targeted mutagenesis of the murine IRP1 and IRP2 genes reveals context-dependent RNA processing differences *in vivo*. *RNA* **10,** 1019–1025
37. Crooks, D.R., Ghosh, M.C., Haller, R.G., Tong, W.H., and Rouault, T.A. (2010) Posttranslational stability of the heme biosynthetic enzyme ferrochelatase is dependent on iron availability and intact iron-sulfur cluster assembly machinery. *Blood* **115,** 860–869
38. Ye, H., and Rouault, T. A. (2010) Human iron-sulfur cluster assembly, cellular iron homeostasis, and disease. *Biochemistry* **49,** 4945–4956
39. Schranzhofer, M., Schifrer, M., Cabrera, J. A., Kopp, S., Chiba, P., Beug, H., and Müllner, E. W. (2006) Remodeling the regulation of iron metabolism during erythroid differentiation to ensure efficient heme biosynthesis. *Blood* **107,** 4159–4167
40. Pondarré, C., Antiochos, B. B., Campagna, D. R., Clarke, S. L., Greer, E. L., Deck, K. M., McDonald, A., Han, A. P., Medlock, A., Kutok, J. L., Anderson, S. A., Eisenstein, R. S., and Fleming, M. D. (2006) The mitochondrial ATP-binding cassette transporter Abcb7 is essential in mice and participates in cytosolic iron-sulfur cluster biogenesis. *Hum. Mol. Genet.* **15,** 953–964
41. Csere, P., Lill, R., and Kispal, G. (1998) Identification of a human mitochondrial ABC transporter, the functional orthologue of yeast Atm1p. *FEBS Lett.* **441,** 266–270
42. Cavadini, P., Biasiotto, G., Poli, M., Levi, S., Verardi, R., Zanella, I., Derosas, M., Ingrassia, R., Corrado, M., and Arosio, P. (2007) RNA silencing of the mitochondrial ABCB7 transporter in HeLa cells causes an iron-deficient phenotype with mitochondrial iron overload. *Blood* **109,** 3552–3559
43. Tong, W. H., and Rouault, T. (2000) Distinct iron-sulfur cluster assembly complexes exist in the cytosol and mitochondria of human cells. *EMBO J.* **19,** 5692–5700
44. Kispal, G., Csere, P., Prohl, C., and Lill, R. (1999) The mitochondrial proteins Atm1p and Nfs1p are essential for biogenesis of cytosolic Fe/S proteins. *EMBO J.* **18,** 3981–3989
45. Wang, Y., Langer, N. B., Shaw, G. C., Yang, G., Li, L., Kaplan, J., Paw, B. H., and Bloomer, J. R. (2011) Abnormal mitoferrin-1 expression in patients with erythropoietic protoporphyria. *Exp. Hematol.* **39,** 784–794
46. Whatley, S. D., Ducamp, S., Gouya, L., Grandchamp, B., Beaumont, C., Badminton, M. N., Elder, G. H., Holme, S. A., Anstey, A. V., Parker, M., Corrigall, A. V., Meissner, P. N., Hift, R. J., Marsden, J. T., Ma, Y., Mieli-Vergani, G., Deybach, J. C., and Puy, H. (2008) C-terminal deletions in the ALAS2 gene lead to gain of function and cause X-linked dominant protoporphyria without anemia or iron overload. *Am. J. Hum. Genet.* **83,** 408–414
47. Bishop, D. F., Tchaikovskii, V., Hoffbrand, A. V., Fraser, M. E., and Margolis, S. (2012) X-linked sideroblastic anemia due to carboxyl-terminal ALAS2 mutations that cause loss of binding to the β-subunit of succinyl-CoA synthetase (SUCLA2). *J. Biol. Chem.* **287,** 28943–28955
48. To-Figueras, J., Ducamp, S., Clayton, J., Badenas, C., Delaby, C., Ged, C., Lyoumi, S., Gouya, L., de Verneuil, H., Beaumont, C., Ferreira, G. C., Deybach, J. C., Herrero, C., and Puy, H. (2011) ALAS2 acts as a modifier gene in patients with congenital erythropoietic porphyria. *Blood* **118,** 1443–1451
49. Kadirvel, S., Furuyama, K., Harigae, H., Kaneko, K., Tamai, Y., Ishida, Y., and Shibahara, S. (2012) The carboxy-terminal region of erythroid-specific 5-aminolevulinate synthase acts as an intrinsic modifier for its catalytic activity and protein stability. *Exp. Hematol.* **40,** 477–486
50. Balwani, M., Doheny, D., Bishop, D.F., Nazarenko, I., Yasuda, M., Dailey, H.A., Anderson, K.E., Bissell, D.M., Bloomer, J., Bonkovsky, H.L., Phillips, J.D., Liu, L., Desnick, R.J., and Porphyrias Consortium of the National Institutes of Health Rare Diseases Clinical Research Network (2013) Loss-of-function ferrochelatase and gain-of-function erythroid-specific 5-aminolevulinate synthase mutations causing erythropoietic protoporphyria and x-linked protoporphyria in North American patients reveal novel mutations and high prevalence of X-linked protoporphyria. *Mol. Med.* **19,** 26–35